

Response to reviewers' comments on the manuscript "Satellite observations of stratospheric hydrogen fluoride and comparisons with SLIMCAT calculations" by

Jeremy J. Harrison et al.

We thank the reviewers for their comments. These comments are reproduced below in bold text, followed by our responses.

Reviewer #1:

This is a nice and generally well written paper adding more evidence to the role of dynamics for trends of trace gases in the stratosphere. The authors use here observations of the gas HF and its source gases to compare them with results of the SLIMCAT model. As shown in previous papers with a similar purpose, the sophisticated interplay of dynamics and chemistry does not allow to relate observed stratospheric trends directly with tropospheric emission scenarios. Instead, applying a full chemistry transport model as a first step allows to test if or not data are, in a statistical sense, in agreement with a model simulation. The gas HF allows to study this question for a rather long period, as global observations date back to the HALOE instrument.

On the other hand, I have some comments to the paper which the authors may consider for an improved version:

As a major comment, it is somewhat unclear for me what the original contribution of the authors to the content of the paper is.

We are unsure what point the reviewer is trying to make here, particularly as the author contributions are listed in the 'Author contribution' section of the manuscript. We suspect the reviewer is asking for a clearer statement of the new science in the paper, which we have tried to provide.

A rather long part of the paper deals with the description of the ACE-FTS HF observations and some discussion of the error budget. Tables 1-3 also add to the impression, that the authors here present for the first time the version 3.0/3.5 retrieval of the HF data.

ACE-FTS HF v3.0 data have appeared in the literature several times before. However, this is the first paper dedicated to investigating an almost complete ACE time series (2004 to 2012), and providing detailed comparisons with a state-of-the-art CTM. We believe this is the first paper to present v3.5 HF data (data from October 2010).

This paper is a sequel to a previous paper on COF₂, and in keeping with this previous paper it was decided to provide a similar amount of detail on the retrieval. Note that the HF and COF₂ retrievals are distinct, with different microwindow sets and different interferers, so this is not simply repetition.

The inclusion of the HALOE dataset on the other hand directs to the presentation of a new combined dataset. Indeed, the authors present here for the first time (as I understand) the GOZCARDS data set of HF, but which is from version 2.2 of ACE-FTS.

Yes, we are presenting the GOZCARDS HF data for the first time. We have now mentioned this point in the text.

For the model simulation, there is a similar question if the data presented in the paper are from the same run as used in the paper Harrison et al., 2014, or if a different setup has been used. So my strong suggestion would be to state clearly what original new contributions have been made for this paper and how this differs to previous work.

This work does use SLIMCAT data from a new run. The most important update for this new run is that the photolysis scheme now uses modelled ozone profiles in each grid box instead of climatological ozone profiles. We have described these differences, but note that the effects are small and this is not a major scientific point.

In this line, the paper is in my opinion undecided over its focus. In case the data are in the focus, I would expect to see more of validation work or the construction of a new combined data set. In case atmospheric processes is in the focus, I would expect to see a deeper discussion of the relation between HF and its direct precursors COF₂ and COClF (eg. seasonal plots), as an extension of the correlation plots. In case the evaluation of atmospheric transport is in the focus, comparison with tracers of transport (at least for the model) and their discussion would be necessary.

The focus of this work is not 'data'. We will include more of a discussion on model COF₂ and COClF for completeness. The main science we will expand upon is on the stratospheric transport (see response to Reviewer #2).

Minor comments:

As solar occultation data are sparse, there may be selection effects when comparing zonal means from different data sets and model. This effect may be especially important in high latitude spring when strong azonal structures may develop. Does this explain the higher seasonal amplitude at high latitudes? In principle, one could, as a first step, use co-located data from model and observations. Have you checked if this would change the trend analysis?

The ACE-FTS takes many measurements at high latitudes, so we do not expect any selection effects due to sparsity of data in high latitude spring. The difference in seasonal amplitude between observation and model is real.

The SLIMCAT model has an upper boundary of 60 km. The stratospheric maximum may not be well presented in the model and HF depleted mesospheric air in polar spring cannot be reproduced by the model. Do you see such effects and does it have any implication for your analysis?

According to Ricaud and Lefevre (referenced in the manuscript), some HF is transported up into the mesosphere, where its mixing ratio remains constant up to high altitudes. At the poles, data are only available up to ~ 50 km. If HF were depleted high up via dissociation, when the air descended the F atoms would simply reform HF. At the 50 – 60 km level, we see no evidence for any depletion.

p34380 l 17: In Fig. 6, at 44.5 km model and HALOE converge, esp. at high lat, meaning that they have a different trend. In Fig 7. they seem to agree perfectly. This looks like more than just a bias shift.

There are some minor differences in how the HALOE data were filtered at high latitudes and altitudes, so there are some minor differences in addition to a simple bias shift. The reviewer is exaggerating when claiming in Fig. 7 'they seem to agree perfectly'; there is no perfect agreement between model and observation.

p34375 l11: compare lifetime of COClF with p34365 l13. Did you re-determine its value

here?

Yes, it has been re-calculated for this work. The COF₂ SLIMCAT lifetime has also been updated (due to the photolysis change) and will be included in the manuscript.

p34371 I24: see Waymark et al., 2013, ANNALS OF GEOPHYSICS, 56, Fast Track-1, 2013; 10.4401/ag-6339

There is nothing new in the Waymark paper. The information is taken directly from the Duchatelet paper, which we reference.

Typos or similar:

p34366 I17: Jungfraujoch observations are remote sensing, too. I23: the "however" sounds strange for me when it relates to the space shuttle.

The language has been tidied up here. Although there are some measurements from the space shuttle, these do not provide global coverage over long time periods.

Reviewer #2:

In this manuscript, the authors combine the two multi-year satellite infrared solar occultation data sets available for hydrogen fluoride (HF), the main stratospheric reservoir of fluorine, in order to determine its global distribution and trend over the 1991-2012 time frame. The version 19 set (the latest release to my knowledge) derived from the HALOE (HALogen Occultation Experiment) observations and covering the 1991-2005 period is used, complemented with several subsets (v2.2, v3 and v3.5) derived from the ACE (Atmospheric Chemistry Experiment)-FTS instrument, in operation since 2004.

We wish to point out that the GOZCARDS HF data product was not created specifically for this work. Here we only make use of *existing* HF datasets.

Furthermore, ACE-FTS data available for the main F-bearing source gases (CFC-12, CFC-11 and CFC- 113) and two intermediates of their degradation (COF₂ and COClF) are presented. Model results by the TOMCAT/SLIMCAT 3D Chemical Transport Model are included for comparison with the observations and to support the interpretation of the results.

The manuscript is generally clear and well written (although some figures (as Fig. 6) remain tiny and of limited use), the data sets and the results are important and the subject is clearly of relevance for this journal. In my opinion, there are however a few drawbacks that need to be fixed before publication. They are identified and listed below, together with suggestions for improvement.

While one of the aim of this paper is to characterize and understand the evolution of HF over two decades or so, with two different instruments (already a challenge with only a few months overlap between the two missions...), three -possibly inconsistent!- versions of the ACE-FTS data are used, version 2.2, version 3 and 3.5. Moreover, these versions are incompletely described, with e.g., Table 1, 2 and 3 providing information as to the settings for v3 and v3.5, but nothing for v2.2. There is no effort to characterize a possible systematic bias (because different HF lines might be used, the interferences accounted for might be dissimilar...) and to merge the ACE data sets.

All ACE v3.0 data from October 2010 suffer from problems in the P and T supplied by the Canadian Meteorological Centre, and are therefore unusable. V3.5 remedies this problem by

using the correct P and T; in this work we use v3.5 data for measurements taken from October 2010. The retrieval schemes are identical. We will explain this more clearly in the manuscript.

It is not possible to characterise a systematic bias between these datasets, only a relative bias. There is no bias between v3.0 and v3.5 (it is the same retrieval), and v3.0/v3.5 and v2.2 agree within $\pm 5\%$; this has been added to the manuscript. We believe that v3.0/v3.5 is an improvement relative to v2.2. There are undoubtedly biases between the nineteen different HALOE data versions, but it is considered that the latest, v19, is the most reliable. We do not understand how merging different ACE datasets will be beneficial; it is not something that is generally done.

The same is true for the combination of ACE-FTS with HALOE results, despite a well-known bias. The authors state (section 3.2, page 34371): "There have been no detailed comparisons in the literature between ACE-FTS v2.2 and v3.0 HF datasets, however Duchatelet et al. (2010) state that first comparison exercises involving ACE-FTS v3.0 products indicate a decrease of close to 5% in HF amounts". If the bias is not well known while perhaps non-negligible (5%), the authors have to characterize it, this is certainly not beyond the scope of this study, given its aims. They have at hand all what is needed and my recommendation is to use significant subsets of occultations available for v2.2, v3 and v3.5 to determine their consistency and correct for a possible systematic bias. The next step will require a careful combination with the HALOE set, following e.g. the method developed for the generation of the GOZCARDS data product.

As explained in the responses to Reviewer #1, this paper is not focussed on data and the process of combining datasets. We make use of *existing* HF datasets in order to derive trends and information on HF in the atmosphere.

Note that the merging process does not correct for any systematic bias between HALOE and ACE-FTS datasets, only for the relative bias. We have compared the ACE-FTS HF v3.0/v3.5 and v2.2 datasets and found them to agree within $\pm 5\%$. The bias of 5% discussed in Duchatelet et al. (2010) does not appear to be correct.

In the present version of the manuscript, the GOZCARDS ensemble appears useless or underutilized. Added "for completeness" (section 2.3, page 34370), it is only included in Figure 7 and little is learnt from these comparisons. Indicatively, neither the abstract nor the conclusions mention findings resulting from its use. The statement on page 34380-34381 "Had v3.0/v3.5 ACE data been used instead, the GOZCARDS dataset would have been shifted lower in VMR by several percent" further adds to the confusion, leaving the reader unsure about the consistency of the data sets used for the trend evaluation. Trend evaluations which btw do not consider the GOZCARDS merged data set, while it is covering the 1991-1997, 1998-2005 and nearly the 2004-2012 (2004-2010) time intervals. Therefore, my recommendation would be either to discard the GOZCARDS set (saving one figure), or to keep and exploit a merged set for the trend investigations, i.e. supposedly an asset with this respect.

The inclusion of GOZCARDS HF data was simply to ascertain how well a merged dataset would compare with SLIMCAT. There is discussion in the manuscript on comparisons between SLIMCAT and GOZCARDS. Trends were not calculated using GOZCARDS because a merged dataset, which is related to each of the original datasets by a simple multiplicative factor, should produce trends that are the same or at least very similar. The reviewer has mentioned that we need to correct the systematic bias, however it must be stressed that a merged HALOE-ACE dataset only corrects for a relative bias. Any future GOZCARDS HF product using the same v19 HALOE but a different ACE dataset version

will be very similar to the current product, but with a small relative bias. There is still no information as to which is the more accurate. The statement on lines 34380-34381 has been removed. We have also removed the words “for completeness”.

One of the conclusions of this study is that changes or variability in stratospheric dynamics are responsible of variations in the HF trends with altitude and latitude. Several recent papers have identified and investigated these changes (e.g. Ploeger et al., 2015, doi:10.1002/2014JD022468, a reference to it might be useful to the reader), or their impact on significant stratospheric composition changes with time (e.g. for ozone, hydrogen chloride...). As a possible result, the evolution of HF in the stratosphere might well not always follow a smooth route, as is the case in the troposphere, complicating the interpretation of its trend in the stratosphere (upper or lower, in SH or NH), to e.g. support the Montreal Protocol. Indeed, how are the circulation changes and the reduction/variation in source gases emissions contributing to the derived trends? I believe it is therefore important to provide elements allowing to fully characterize these contributions.

Yes, this is a good point. We are aware of papers which have pointed out recent variations in stratospheric circulation – in addition to the Ploeger paper there is one by Mahieu et al. ([doi:10.1038/nature13857](https://doi.org/10.1038/nature13857)), which discussed HCl. The modelling in these studies is based on dynamical variability as diagnosed the ECMWF ERA-Interim reanalyses, which are also used in this study. We have added a discussion of these points and mentioned the consistency between the observed HF variability and the other sources of information. We have also shown more results from the fixed dynamics SLIMCAT run (see next point).

The support of SLIMCAT is key here, and the figure 8 (and similar) provide an important input, showing the net and contrasted effect of stratospheric dynamics on the HF trend over the 2004-2012 time period. But there is no information as to the temporal development of HF with altitude/latitude. I think that adding the "fixed to 2000 dynamics" SLIMCAT time series to Figure 6 would be very useful to identify in the various subsets the most significant departures from a smooth unperturbed HF evolution as driven only by surface emissions of the source gases and their subsequent conversion to inorganic fluorine.

The fixed SLIMCAT data has been added as requested.

Minor comments/corrections

Abstract

P34363-L3: suggest adding "involving" to get "...nature, involving e.g. chlorofluorocarbons (CFCs),..."

We are not convinced that this will improve the text.

Introduction

P34364-L7: "source molecules are CFC-12, CFC-11, CFC-113" instead of "source molecules are CFC-11, CFC-12, CFC-113"

The change has been made.

P34364-L16: suggest changing to "Certainly, in addition of HCl, monitoring the growth..."

We have added “(in addition to monitoring stratospheric HCl)” to the end of this sentence.

P34365-L5: suggest adding a blank line between R2 and R3

This is a type-setting issue. The original submission does have a blank line here.

P34366-L15: suggest changing to "..., based on solar spectra recorded by balloonborne and from the ground at Jungfraujoch,"

This has been changed to "... based on solar spectra recorded from balloon and on the ground at Jungfraujoch,"

Section 2.1

P34368-L22: change to "an atmospheric density of 9E15 or 2E16 molecules cm-3"

The text is correct as is. The upper altitude of the retrieval corresponds with the lower atmospheric density (9E15 molecules cm⁻³).

Section 2.2

P34369-L19: Change to "For the HF channel, the spectral bandpass..."

This has been done.

Section 3.1

P34371: I am questioning the relevance and usefulness of the paragraph between lines 8 and 14, starting at "Recently"

This paragraph explains a source of error in the HF spectroscopic line parameters used in this work. The air-broadening parameters were derived using the Galatry lineshape, but these values were attributed to the Voigt lineshape when added into HITRAN.

Section 4

P34374-L12: Could the switch from ECMWF to ERA-I reanalyses be responsible of a bias/change in quality in the SLIMCAT simulations? With a significant impact on the respective HF trends?

The switch actually occurs on 1/1/1979, not 1/1/1989. We apologise for the typo in the text but the earlier 10 years of ERA-I were produced by ECMWF after the main processing and some earlier SLIMCAT runs did change in 1989. We have corrected the date in the text. In any case, even 1/1/1989 is significantly before the start of the analysis period and this provides a long enough spin up. The period analysed is all based on consistent ERA-I winds.

Section 6

P34383-L7: a reference such as Ploeger et al. JGR, 2015 might be relevant/useful here OK.

Table 1. Wouldn't it be more useful to quote the upper approximate altitudes in the last column, for all cases, and mention the density unit threshold in the foot note for the relevant cases?

This is in keeping with the official ACE-FTS microwindow document.

Figure 7: the GOZCARDS symbol should be "empty" (instead of a black diamond)

We have remade the plot with empty diamonds.

27 June 2016

Deleted: 22 October

Deleted: 5

Satellite Observations of Stratospheric Hydrogen Fluoride and Comparisons with SLIMCAT Calculations

by

Jeremy J. Harrison^{1,2}, Martyn P. Chipperfield^{3,4}, Christopher D. Boone⁵, Sandip S. Dhomse^{3,4}, Peter F. Bernath⁶, Lucien Froidevaux⁷, John Anderson⁸, and James Russell III⁸

¹Department of Physics and Astronomy, University of Leicester, [Leicester LE1 7RH, United Kingdom](#).

Deleted: University Road,

²National Centre for Earth Observation, University of Leicester, [Leicester LE1 7RH, United Kingdom](#).

Deleted: University Road,

³Institute for Climate and Atmospheric Science, School of Earth and Environment, University of Leeds, [Leeds LS2 9JT, United Kingdom](#).

Deleted: .

⁴National Centre for Earth Observation, School of Earth and Environment, University of Leeds, [Leeds LS2 9JT, United Kingdom](#).

Deleted: .

⁵Department of Chemistry, University of Waterloo, [Waterloo, Ontario N2L 3G1, Canada](#).

Deleted: 200 University Avenue West

⁶Department of Chemistry and Biochemistry, Old Dominion University, Norfolk, Virginia 23529, United States of America.

⁷Jet Propulsion Laboratory, Pasadena, California [91109](#), United States of America.

⁸Department of Atmospheric and Planetary Sciences, Hampton University, [Hampton, Virginia 23668](#), United States of America.

Number of pages = 30

Deleted: 29

Number of tables = 5

Number of figures = 11

Deleted: 0

Address for correspondence:

Dr. Jeremy J. Harrison
National Centre for Earth Observation
Department of Physics and Astronomy
University of Leicester
University Road
Leicester LE1 7RH
United Kingdom

Tel: (44)-116-2231943

e-mail: jh592@leicester.ac.uk

48 **Abstract**

49 The vast majority of emissions of fluorine-containing molecules are anthropogenic
50 in nature, e.g. chlorofluorocarbons (CFCs), hydrochlorofluorocarbons (HCFCs), and
51 hydrofluorocarbons (HFCs). Many of these fluorine-containing species deplete stratospheric
52 ozone, and are regulated by the Montreal Protocol. Once in the atmosphere they slowly
53 degrade, ultimately leading to the formation of HF, the dominant reservoir of stratospheric
54 fluorine due to its extreme stability. Monitoring the growth of stratospheric HF is therefore
55 an important marker for the success of the Montreal Protocol.

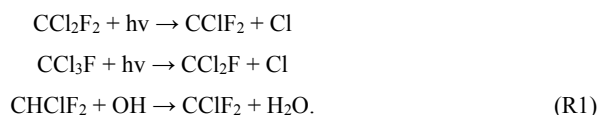
56 We report the comparison of global distributions and trends of HF measured in the
57 Earth's atmosphere by the satellite remote-sensing instruments ACE-FTS (Atmospheric
58 Chemistry Experiment Fourier Transform Spectrometer), which has been recording
59 atmospheric spectra since 2004, and HALOE (HALogen Occultation Experiment), which
60 recorded atmospheric spectra between 1991 and 2005, with the output of SLIMCAT, a state-
61 of-the-art three-dimensional chemical transport model. In general the agreement between
62 observation and model is good, although the ACE-FTS measurements are biased high by
63 ~10% relative to HALOE. The observed global HF trends reveal a substantial slowing down
64 in the rate of increase of HF since the 1990s: 4.97 ± 0.12 %/year (1991-1997; HALOE), 1.12
65 ± 0.08 %/year (1998-2005; HALOE), and 0.52 ± 0.03 %/year (2004-2012; ACE-FTS). In
66 comparison, SLIMCAT calculates trends of 4.01 %/year, 1.10 %/year, and 0.48 %/year,
67 respectively, for the same periods; the agreement is very good for all but the earlier of the
68 two HALOE periods. Furthermore, the observations reveal variations in the HF trends with
69 latitude and altitude, for example between 2004 and 2012 HF actually decreased in the
70 southern hemisphere below ~35 km. An additional SLIMCAT simulation with repeating
71 meteorology for the year 2000 produces much cleaner trends in HF with minimal variations
72 with latitude and altitude. Therefore, the variations with latitude and altitude in the observed
73 HF trends are due to variability in stratospheric dynamics on the timescale of a few years.
74 Overall, the agreement between observation and model points towards the ongoing success of
75 the Montreal Protocol and the usefulness of HF as a metric for stratospheric fluorine.

76

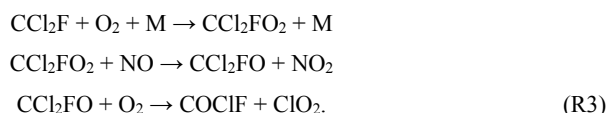
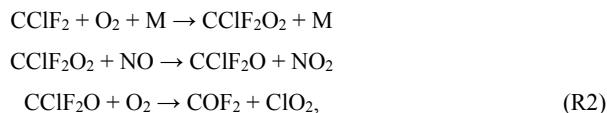
1. Introduction

The accumulation of fluorine in the Earth's atmosphere has resulted from anthropogenic emissions of organic molecules such as chlorofluorocarbons (CFCs), hydrochlorofluorocarbons (HCFCs), and hydrofluorocarbons (HFCs). The long atmospheric lifetimes of such molecules allow them to reach the stratosphere, where they break down and liberate fluorine in various inorganic forms. The most abundant of the emitted organic source molecules are ~~CFC-12 (CCl₂F₂), CFC-11 (CCl₃F), CFC-113 (CCl₂FCClF₂),~~ which are all now banned under the Montreal Protocol because they deplete stratospheric ozone, and HCFC-22 (CHClF₂), the most abundant HCFC and a transitional substitute under the Protocol. Although long-lived, these molecules do degrade in the atmosphere at high altitudes, ultimately to the long-lived stratospheric reservoir molecule hydrogen fluoride, HF; the chemistry schemes are presented below. Monitoring HF as part of the atmospheric fluorine family is important in closing the fluorine budget, particularly as anthropogenic emissions of fluorine species, many of which are ozone-depleting and all of which are greenhouse gases, have varied substantially over time. Certainly, monitoring the growth of stratospheric HF, which has slowed in recent years, is an important marker for the success of the Montreal Protocol [\(in addition to monitoring stratospheric HCl\)](#).

For the three most abundant fluorine source gases, CFC-12, CFC-11, and HCFC-22, atmospheric degradation proceeds with the breaking of a C-Cl (CFC-12 and CFC-11) or C-H (HCFC-22) bond (Ricaud and Lefevre, 2006),



Depending on their structure, the intermediates produced in R1 react further,



Deleted: CFC-12 (CCl₂F₂),

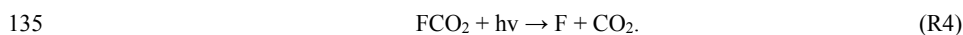
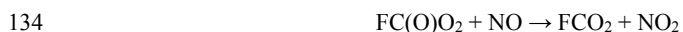
112

113 For CFC-113, and minor sources such as HFCs (e.g. HFC-134a, HFC-152a), the reaction
114 scheme is similar.

115 In Equations R2 and R3, carbonyl chloride fluoride (COCIF) and carbonyl fluoride
116 (COF_2), are important ‘inorganic’ reservoirs (the common terminology in atmospheric
117 science differs from that in chemistry) of fluorine in the stratosphere, with lifetimes of 1.6
118 (Fu et al., 2009) and 3.8 (Harrison et al., 2014) years, respectively; COF_2 is more abundant
119 than COCIF. The trends in these inorganic reservoirs over time are directly related to the
120 trends of the individual source gases. The decrease in the amounts of atmospheric CFC-11
121 and CFC-113, the principal sources of carbonyl chloride fluoride, has led to a decreasing
122 trend in this reservoir (Brown et al., 2011), whereas carbonyl fluoride is still slowly
123 increasing over time due to the increase in HCFC-22, which more than compensates for the
124 decrease in the CFC-12 and CFC-113 source gases (Brown et al., 2011; Harrison et al.,
125 2014).

126 COCIF and COF_2 volume mixing ratios (VMRs) slowly increase with altitude
127 through the lower stratosphere until they reach their respective maxima, at ~25 – 30 km for
128 COCIF (Fu et al., 2009) and ~30 – 40 km for COF_2 (Harrison et al., 2014). Above these
129 altitudes photolysis becomes more efficient, leading to the formation of fluorine atoms,

130



136

137 The liberated fluorine atoms then react with methane, water or molecular hydrogen, to form
138 the inorganic product hydrogen fluoride, HF. At the top of the stratosphere most of the
139 fluorine is present as HF (Brown et al., 2014), the dominant reservoir of stratospheric
140 fluorine due to its extreme stability. Note that due to this stability, F is not important for
141 catalytic stratospheric ozone loss. HF is removed from the stratosphere by slow transport to,
142 and rainout in, the troposphere, or by upward transport to the mesosphere, where it is
143 destroyed by photolysis (Duchatelet et al., 2010). Overall the amount of HF in the
144 atmosphere is increasing (e.g. Brown et al., 2014).

145 The first detection of HF in the Earth's stratosphere, based on solar spectra recorded
146 ~~from~~ balloon, and ~~on the~~ ground, at Jungfraujoch, was made by Zander et al. (1977).
147 Measurements continue to be made at Jungfraujoch using a ground-based Fourier transform
148 spectrometer (FTS), (e.g. Duchatelet et al., 2010). There have also been ~~measurements~~ of HF
149 taken, for example, by the Atmospheric Trace MOlecule Spectrometry Experiment
150 (ATMOS) instrument which flew four times on NASA Space Shuttles between 1985 and
151 1994 (Irion et al., 2002) and the MkIV interferometer, a balloon-borne solar occultation FTS
152 (Velazco et al., 2011). Measurements taken by satellite-borne instruments, however, allow
153 HF to be observed with global coverage, and seasonal and latitudinal variability to be
154 investigated fully. The first global atmospheric distributions of HF were provided by the
155 HALogen Occultation Experiment (HALOE) instrument, onboard the Upper Atmosphere
156 Research Satellite (UARS), which recorded atmospheric spectra between 1991 and 2005.
157 More recently, the Atmospheric Chemistry Experiment (ACE)-FTS, onboard the SCISAT
158 satellite, has been recording atmospheric spectra since 2004, carrying the mantle of HF
159 measurements into the second decade of the twenty-first century. In fact, the ACE-FTS is the
160 only satellite instrument currently taking measurements of HF.

161 This paper follows on from our recent work on the global distributions and trends of
162 COF₂, the most important 'temporary' stratospheric fluorine reservoir that directly leads to
163 the formation of HF. The aim of the present work is to understand the HF global distribution
164 and trends derived from satellite observations taken by the HALOE and ACE-FTS
165 instruments. To do this, we use the SLIMCAT model, a state-of-the-art three-dimensional
166 (3D) chemical transport model (CTM), one of the few to include stratospheric fluorine
167 chemistry. Additionally, we compare tracer-tracer correlations between some of the major
168 HF 'sources' for SLIMCAT and satellite observations as a further test of the model
169 chemistry.

170

171 **2. Hydrogen fluoride datasets**

172 **2.1. ACE-FTS**

173 The ACE-FTS instrument, which covers the spectral region 750 to 4400 cm⁻¹ with a
174 maximum optical path difference (MOPD) of 25 cm and a resolution of 0.02 cm⁻¹ (using the
175 definition of 0.5/MOPD throughout), uses the sun as a source of infrared radiation to record
176 limb transmission through the Earth's atmosphere during sunrise and sunset ('solar
177 occultation'). Transmittance spectra are obtained by ratioing against exo-atmospheric 'high
178 sun' spectra measured each orbit. These spectra, with high signal-to-noise ratios, are

Deleted: by

Deleted: -borne

Deleted: -based solar spectra

Deleted: remote-sensing

183 recorded through long atmospheric limb paths (~300 km effective length), thus providing a
184 low detection threshold for trace species. ACE has an excellent vertical resolution of about
185 3-4 km and can measure up to 30 occultations per day, with each occultation sampling the
186 atmosphere from 150 km down to the cloud tops (or 5 km in the absence of clouds). The
187 locations of ACE occultations are dictated by the low Earth circular orbit of the SCISAT
188 satellite and the relative position of the sun. Over the course of a year, the ACE-FTS records
189 atmospheric spectra over a large portion of the globe (Bernath et al., 2005), from which it is
190 possible to extract profiles of many fluorine-containing species, including CCl₃F (CFC-11),
191 CCl₂F₂ (CFC-12), CHClF₂ (HCFC-22), CCl₂FCClF₂ (CFC-113), CH₃CCl₂F (HCFC-141b),
192 CH₃CClF₂ (HCFC-142b), CH₂FCF₃ (HFC-134a), CHF₃ (HFC-23), CF₄, COF₂, COClF, HF
193 and SF₆.

194 The atmospheric pressure and temperature profiles, the tangent heights of the
195 measurements, and the hydrogen fluoride VMRs were taken from version 3.0 (January 2004
196 until September 2010) and v3.5 (from October 2010) processing of the ACE-FTS data. Note
197 that the retrieval scheme is identical for both the v3.0 and v3.5 datasets, the difference being
198 in the meteorological data used as input for the pressure and temperature retrievals (the
199 lowest ACE-FTS levels use these data directly). Due to an error in these inputs, v3.0 data
200 should only be used for measurements taken until the end of September 2010, while v3.5 is
201 valid for all ACE-FTS measurements. Details of the retrieval scheme for versions 3.0/3.5
202 processing have been explained elsewhere (e.g., Boone et al., 2013; Harrison et al., 2014).
203 Briefly, vertical profiles of trace gases (along with temperature and pressure) are derived
204 from the recorded transmittance spectra via an iterative Levenberg-Marquardt nonlinear
205 least-squares global fit to the selected spectral region(s) for all measurements within the
206 altitude range of interest. The microwindow set and associated altitude ranges for the HF
207 retrieval are listed in Table 1. The VMRs for molecules with absorption features in the
208 microwindow set (see Table 2) were adjusted simultaneously with the HF amount. All
209 spectroscopic line parameters were taken from the HITRAN 2004 database (Rothman et al.,
210 2005), with HF parameters apparently unchanged since HITRAN 1992. The microwindow
211 set covers eight spectroscopic lines (P₁, P₂, P₃, P₄, R₀, R₁, R₂, R₃) from the fundamental (1-0)
212 band of HF. The HF retrieval extends from a lower altitude of 12 km up to altitudes
213 corresponding to an atmospheric density of 9.0×10^{15} molecules cm⁻³, in practice ~50-55 km,
214 thus providing a variation in upper altitude with both latitude and season (see Table 1). The
215 HF spectral signal in ACE-FTS spectra recorded above the upper altitude retrieval limit is
216 generally below the noise level, so it is not possible to retrieve VMRs directly at these

217 altitudes. Instead, the VMR profile above the highest analysed ACE measurement is
218 calculated by scaling the ‘initial’ VMR profile, taken from ATMOS measurements (Irion et
219 al., 2002), over these altitudes; the scaling factor is determined during the least-squares
220 fitting.

221

222 **2.2. HALOE**

223 Like the ACE-FTS, the HALOE instrument (Russell et al., 1993) used the principle
224 of solar occultation to sound the middle atmosphere at sunset and sunrise (relative to the
225 instrument). HALOE used broadband and gas-filter radiometry, with channels covering
226 selected portions of the spectrum between 2.45 and 10.04 μm , to determine the mixing ratios
227 of molecules related to the chemistry of stratospheric ozone and its destruction by CFCs. In
228 particular, HALOE provided measurements of O_3 , HCl, HF, CH_4 , H_2O , NO, NO_2 , aerosol
229 extinction, and temperature versus pressure, over an altitude range of ~ 15 to 60 – 130 km
230 depending on channel (HF, HCl, CH_4 and NO were measured using gas filter radiometry).
231 As with the ACE-FTS, the locations of HALOE occultations and hence the extent of its
232 global coverage were dictated by its orbit and the relative position of the sun. HALOE, with
233 an orbit inclination of 57° compared with 74° for the ACE-FTS, had a more even latitudinal
234 coverage and provided more data over tropical regions, for example, than the ACE-FTS
235 which takes most of its measurements at high latitude.

236 The atmospheric pressure, temperature, tangent heights, and hydrogen fluoride
237 VMRs were taken from version 19 processing of the HALOE data, which are available from
238 October 1991 to November 2005. The retrieval scheme incorporates a simple ‘onion
239 peeling’ approach stabilised at the top and bottom of the profile with a scalar optimal
240 estimation formulation developed by Connor and Rodgers (1989). [For the HF channel, the](#)
241 spectral bandpass 5% relative response points are 4025 cm^{-1} and 4135 cm^{-1} . The HF spectral
242 line parameters were taken from the HITRAN 1992 database (Rothman et al., 1992). The
243 instantaneous vertical field-of-view in the limb is $\sim 1.6\text{ km}$. Detailed validation studies for
244 HALOE HF measurements were published by Russell et al. (1996). Note that for internal
245 consistency with previous work on the fluorine budget (Brown et al., 2014) and COF_2
246 (Harrison et al., 2014), the vertical pressure grid has been interpolated onto the standard 1-km
247 grid used by the ACE-FTS.

248

249 **2.3. GOZCARDS**

Deleted: T

251 The ACE-FTS, HALOE and SLIMCAT model time series are also compared with
252 those of the GOZCARDS (Global OZone Chemistry And Related Datasets for the
253 Stratosphere) HF data product in Section 5. GOZCARDS provides a global long-term
254 stratospheric Earth System Data Record (ESDR) for stratospheric ozone and related chemical
255 species, including HF. The HF data record was not ready in time to be included in the
256 original dataset provided for public usage (temperature, O₃, H₂O, HCl, N₂O, and HNO₃); we
257 are presenting the HF data for the first time here. Froidevaux et al. (2015) have described the
258 GOZCARDS data creation methodology and some stratospheric characteristics concerning
259 the latter five species. The constituent datasets are time series of monthly zonal means
260 versus latitude (in 10° latitude bins) taken from existing satellite datasets. In particular, the
261 GOZCARDS HF data product is derived by merging the v19 HALOE (1991 – 2005) and
262 v2.2 ACE-FTS (2004 – 2010) datasets, with the relative bias between source datasets
263 removed by averaging them over the overlap period 2004 – 2005 and adjusting the series
264 accordingly; note that such a process does not account for any systematic biases in the
265 original datasets. All GOZCARDS datasets are provided on a vertical pressure grid. Again,
266 to be consistent with previous ACE work, this vertical pressure grid has been interpolated
267 onto the standard 1-km grid used by the ACE-FTS. Note that as this GOZCARDS dataset
268 uses v2.2 ACE-FTS data, the time series terminates in September 2010.

Deleted: For completeness, t

Deleted: ;

Deleted: however, t

270 3. Retrieval errors

271 3.1. Infrared spectroscopy of hydrogen fluoride

272 One of the major sources of systematic error for any retrieved atmospheric profile
273 arises from uncertainties in the laboratory spectroscopic data. A discussion of spectroscopic
274 errors is therefore appropriate. The ACE-FTS retrieval makes use of HF line parameters first
275 made available as part of the HITRAN 1992 database (and remaining unchanged until the
276 HITRAN 2012 release), with partition data taken from the Total Internal Partition Sums
277 (TIPS) subroutine included in the HITRAN compilation. HITRAN simply provides error
278 codes for line parameters in the form of uncertainty ranges, but with no information as to
279 how the parameters are correlated. For the HF line parameters used in this work, the errors
280 correspond to 0.0001 – 0.001 cm⁻¹ for the line wavenumber, ν , 2 – 5 % for the line intensity,
281 S , and 1 – 2 % for the air-broadened half-width, γ_{air} . Errors are unreported for γ_{self} (self-
282 broadened half-width), n_{air} (temperature-dependence exponent for γ_{air}), and δ_{air} (air pressure-
283 induced line shift). Recently, and after v3.0 processing of the ACE data was complete,
284 HITRAN 2012 became available; it includes a complete re-evaluation of HF spectroscopy.

288 The associated publication (Rothman et al., 2013) also explains that all the air-broadening
289 parameters, γ_{air} , for the fundamental band of HF were fitted with the Galatry profile, not the
290 Voigt profile, which is the lineshape of choice for the HITRAN database. Additionally, the
291 Dicke narrowing parameters in the original analysis were simply neglected. For the purposes
292 of this work, we assume a retrieval error of at most $\sim 4\%$ arising from uncertainties in HF
293 line parameters.

294

295 3.2. ACE-FTS

296 The ACE v2.2 HF data product, which uses a slightly different microwindow set
297 from v3.0/v3.5 as well as an earlier version of the PT retrieval, has previously been validated,
298 for example, against measurements taken by HALOE and the MkIV interferometer (Mahieu
299 et al., 2008). It was found that ACE-FTS v2.2 HF measurements are biased high compared
300 to HALOE, with mean differences around 5–20% between 15 and 49 km. Comparison of
301 ACE-FTS v2.2 HF with MkIV data is generally good, with relative differences above 19 km
302 within $\pm 10\%$. There have been no detailed comparisons in the literature between ACE-FTS
303 v2.2 and v3.0 HF datasets, although Duchatelet et al. (2010) suggest that ACE-FTS v3.0 HF
304 VMRs have decreased by close to 5% relative to v2.2. However, a re-evaluation of filtered
305 v2.2 and v3.0/v3.5 HF data carried out as part of this work indicates good agreement within \pm
306 5%, with no significant overall bias between the two datasets.

307 The 1σ statistical fitting errors for a single ACE profile are typically $\sim 5\%$ over most
308 of the altitude range. These errors are random in nature and largely determined by the
309 measurement noise of the ACE-FTS. Averaged profiles tend to be dominated by systematic
310 errors, with random errors reduced by a factor of $1/\sqrt{N}$, where N is the number of profiles
311 averaged. Spectroscopic sources of systematic error predominantly arise from the HF
312 HITRAN linelist ($\sim 4\%$; see Section 3.1), with minor contributions from interfering species
313 that absorb in the microwindow regions; we assume that these contributions are small, at
314 most 1% , due to the lack of systematic features in the spectral residuals (Harrison et al.,
315 2014). Additional systematic errors arise from uncertainties in temperature, pressure, tangent
316 altitude (i.e. pointing) and instrumental line shape (ILS); these were estimated by running the
317 ACE-FTS retrieval for a subset of occultations, with each quantity (b_j) perturbed in turn by
318 its assumed 1σ uncertainty (Δb_j). The fractional retrieval error, μ_j , is defined as

319

Deleted: however

Deleted: state that first comparison exercises involving

Deleted: products indicate a

Deleted: of

Deleted: in HF amounts

325

$$\mu_j = \left| \frac{\text{VMR}(b_j + \Delta b_j) - \text{VMR}(b_j)}{\text{VMR}(b_j)} \right|. \quad (3)$$

326

327 Note that pressure, temperature and tangent height are not strictly independent quantities for
 328 ACE-FTS retrievals; tangent heights are determined from hydrostatic equilibrium, and so
 329 these quantities are strongly correlated. Therefore, only two of these three quantities are
 330 altered: temperature is adjusted by 2 K and tangent height by 150 m (Harrison et al., 2014).
 331 ILS uncertainty is determined by adjusting the field of view by 5 % (Harrison et al., 2014).
 332 A subset of 81 occultations measured between 65° and 70°N in July 2010 was selected for
 333 this analysis. The fractional value estimates of the systematic uncertainties, and their
 334 symbols, are given in Table 3. Assuming uncorrelated quantities, the overall systematic error
 335 in the HF retrieval can be calculated as

336

$$\mu_{\text{systematic}}^2 = \mu_{\text{spec}}^2 + \mu_{\text{int}}^2 + \mu_T^2 + \mu_z^2 + \mu_{\text{ILS}}^2. \quad (4)$$

338

339 The total systematic error contribution to the ACE-FTS HF retrieval is estimated to be ~10 %
 340 over the altitude range of the retrieval.

341 As discussed in Section 3.1, HF VMRs are not directly retrieved for ACE
 342 measurements taken at tangent heights above the upper altitude limits listed in Table 1. In
 343 the ACE-FTS HF retrieval, the calculated spectrum is generated from the sum of
 344 contributions from the tangent layer up to 150 km. For the highest analysed measurement,
 345 the retrieved VMR in the tangent layer is generated from the piecewise quadratic
 346 interpolation scheme (Boone et al., 2013), while the VMR in every layer above that is
 347 determined from scaling the ‘initial’ VMR profile, with the scaling factor determined during
 348 the retrieval by forcing the calculated spectrum to match as best as possible the measured
 349 spectrum for the highest analysed measurement. Since the ‘initial’ profile is fixed to a
 350 constant VMR between 50 and 100 km altitude, and since this portion of the profile is scaled
 351 based on the VMR of the highest analysed ACE measurement, this will likely introduce
 352 systematic errors into the highest altitudes of the retrieved profile. However, since the
 353 scaling factor errors are dominated by the 1σ statistical fitting errors of the highest analysed
 354 ACE measurement, it is anticipated that the systematic errors at the top of the profiles are
 355 reduced when they are averaged to create zonal means.

356

357 **3.3. HALOE**

358 As discussed in Section 3.2, HALOE v19 HF has been validated against ACE-FTS
359 v2.2, with the ACE measurements biased high by around 5–20% between 15 and 49 km
360 (Mahieu et al., 2008). Furthermore, HF data from the MkIV interferometer for three flights
361 (2003 – 2005) agree well with ACE-FTS, with relative differences above 19 km within
362 $\pm 10\%$, suggesting that there is a low bias in HALOE. Detailed HALOE HF error estimates
363 and validation studies have previously been conducted by Russell et al. (1996). The
364 estimated errors range from $\sim 27\%$ at 100 hPa to 15% at 1 hPa. Actual mean differences
365 between HALOE and balloon data from a series of nine FTS under-flights, five operating in
366 the far-IR and four MkIV comparisons in the near-IR, collectively ranged from more than
367 17% below 70 hPa where the mixing ratio is very low to $< 7\%$ above that level, with no
368 positive or negative bias implied. These HALOE data were produced using an early
369 algorithm version, but results have proven to be very stable for later versions.

370

371 **4. TOMCAT/SLIMCAT 3D Chemical Transport Model**

372 SLIMCAT, an off-line 3D CTM, calculates the abundances of a number of
373 stratospheric trace gases from prescribed source-gas surface boundary conditions and a
374 detailed treatment of stratospheric chemistry, including the major species in the O_x , NO_y ,
375 HO_x , F_y , Cl_y and Br_y chemical families (e.g. Chipperfield, 1999; Feng et al., 2007). The
376 model uses winds from meteorological analyses to specify winds and temperatures. This
377 approach gives a realistic stratospheric circulation (Chipperfield, 2006; Monge-Sanz et al.,
378 2007). In the version used here the troposphere is assumed to be well-mixed.

379 For this study SLIMCAT was integrated from 1977 to 2013 at a horizontal
380 resolution of $5.6^\circ \times 5.6^\circ$ and 32 levels from the surface to 60 km. The model uses a σ -p
381 vertical coordinate (Chipperfield, 2006) and was forced by European Centre for Medium-
382 Range Weather Forecasts (ECMWF) reanalyses (ERA-Interim from 1979 onwards). The
383 VMRs of source gases at the surface level were specified using datasets prepared for the
384 WMO/UNEP (2011) ozone assessment. These global mean surface values define the long-
385 term tropospheric source gas trends in the model. Similarly, specification of the surface
386 VMRs of degradation products acts as a sink for these species. The model initialisation used
387 the estimated halocarbon loading for 1977, taken from the WMO/UNEP scenarios.

388 The SLIMCAT run makes use of the same chemistry scheme that was previously
389 used for our work on COF_2 (Harrison et al., 2014), however in the present version the
390 photolysis scheme has been updated to use latitudinally and monthly varying ozone profile

Deleted: 8

Deleted: .

Deleted:

394 shapes in the photolysis look-up table. All source and degradation products related to
395 fluorine chemistry are listed in Table 4. COF₂ contributions arise from the degradation of
396 CFC-12, CFC-113, CFC-114, CFC-115, HCFC-22, HCFC-142b, HFC-23, HFC-134a, HFC-
397 152a, Halon 1211, and Halon 1301, with COCIF production arising from the degradation of
398 CFC-11, CFC-113, and HCFC-141b (CH₃CCl₂F). Some HF is assumed to form directly
399 from the source gases (see Table 4), however this is almost negligible in practical terms (~3
400 % in 2010, mainly arising from HFC-134a). The relative amounts of HF formed (in 2010)
401 via COCIF and COF₂ are 30 and 67 %, respectively.

402 The SLIMCAT calculations reveal that at altitudes above the maximum COCIF and
403 COF₂ VMRs, there is net loss of these at all latitudes. The primary loss of COF₂ and COCIF
404 in the stratosphere occurs via photolysis, with an additional secondary loss mechanism
405 through reaction with O(¹D); SLIMCAT calculates relative contributions of 90 % and 10 %,
406 respectively, for COF₂ (Harrison et al., 2014) and 98 % and 2 % for COCIF. The SLIMCAT
407 outputs enable an estimation of the atmospheric lifetimes of COF₂ and COCIF by dividing
408 the total modelled atmospheric burden of each species by the total calculated atmospheric
409 loss rate. The total calculated mean atmospheric lifetimes are 3.9 years for COF₂, revised
410 upwards from the calculated value of 3.8 years presented by Harrison et al. (2014), and 1.7
411 years for COCIF.

413 5. Comparison between ACE-FTS/HALOE/SLIMCAT datasets

414 The ACE-FTS HF data were binned into five latitude bands by month; VMRs
415 outside six median absolute deviations (MAD) of the median VMR for each bin and altitude
416 were removed from the analysis. Once filtered to remove significant outliers, the data were
417 used to create monthly zonal means at each altitude within 5° latitude bins. In Figure 1 these
418 have been plotted next to SLIMCAT zonal means for the months September 2009 to August
419 2010, thereby revealing the seasonal variation in the HF distribution over this period. Note
420 that these dates have been chosen to match those used in the previous work on carbonyl
421 fluoride (see Figure 11 of Harrison et al., 2014). The HF profiles generally show an increase
422 in VMR with altitude, with the rate of this increase varying with latitude and time of year.
423 Note that ACE-FTS observations do not cover all latitude bins over a single month (see
424 Section 2.1), and that latitude bins containing fewer occultations are noisier in appearance.
425 Despite these caveats, Figure 1 reveals a good agreement between the ACE-FTS observations
426 and the model which reproduces very well the significant seasonal variation. For example,
427 note in particular the agreement for regions of low HF VMR (< 1000 ppt) at ~30 – 40 km

Deleted: .

Deleted: 8

Formatted: Subscript

Deleted: (

Deleted: ,

Deleted: , respectively

433 over the southern tropics in February 2010 and the northern tropics in August 2010; at
434 southern mid- to high-latitudes in December 2009, and March and August 2010; and at
435 northern mid- to high-latitudes in February and March 2010.

436 Plots of ACE-FTS and HALOE HF observations side-by-side with SLIMCAT HF
437 calculations for September 2004 to August 2005 are shown in Figure 2. As for Figure 1, the
438 agreement between observations and model is generally good and the significant seasonal
439 variation is well reproduced. Note that, as for the ACE-FTS, HALOE data do not cover all
440 latitude bins in a given month, although HALOE does take more measurements at lower
441 latitudes. One noticeable difference revealed in Figure 2 is the relative low bias of HALOE
442 measurements compared with ACE-FTS and SLIMCAT; this is most notable at the top of the
443 altitude range. Using the period of overlap between ACE and HALOE, we can estimate that
444 ACE v3.0 is biased high by about 10% relative to HALOE. Biases between observations and
445 SLIMCAT will be more fully addressed in Section 6.

446 The overall atmospheric distribution of HF is determined by a complicated
447 combination of its production and transport, which depends on the production and lifetimes
448 of its ‘sources’ COF₂ and COClF. Figure 3 shows the observed and modelled COF₂ and
449 COClF zonal means for October 2009, and February and August 2010. Due to the upwelling
450 of relatively organic-fluorine-rich air in the tropical regions, the largest VMRs of COF₂ and
451 COClF are found over the tropics (Harrison et al., 2014; Fu et al., 2009), where solar
452 insolation is highest due to the small solar zenith angle, at altitudes of ~30 – 40 and ~25 – 30
453 km. For COF₂ the model agrees well with the ACE observations in terms of magnitude and
454 spatial distribution. For COClF the modelled distribution agrees with ACE but the peak
455 VMR is overestimated. Analysis of the SLIMCAT simulation shows that there is net loss of
456 COF₂ and COClF at altitudes above those of the maximum VMRs, at all locations. There is
457 therefore a correlation between the stratospheric regions of low HF VMR (< 1000 ppt) above
458 ~20 km at the poles and ~25 km at the equator and those of peak COF₂ and COClF VMRs.

459 Figure 1 reveals an asymmetry in the seasonal HF distribution between the two
460 hemispheres. This is attributable to asymmetries in the distributions of the ‘sources’ COF₂ /
461 COClF and their precursors, due to differences in the meridional Brewer-Dobson circulation,
462 and to the stronger descent of air associated with the winter polar vortex in the southern
463 hemisphere; for example, compare the enhanced ACE-FTS HF VMRs near the southern pole
464 in August 2010 with those near the northern pole in February 2010 at ~25 km. An additional
465 source of asymmetry in the COF₂ distribution, which directly influences the HF distribution,
466 arises from the temperature-dependent loss reaction of the COF₂-precursor CHClF₂ (HCFC-

Deleted: 2b

Deleted: er

Deleted: F

Deleted: km

Deleted: ,

Formatted: Subscript

Deleted: i

Deleted: F

474 22) with OH, leading to a secondary COF₂ maximum at southern hemisphere high-latitudes
475 in the summer mid-stratosphere (~10 K warmer than the corresponding location in the
476 northern hemisphere) (Harrison et al., 2014); for example, compare the ACE-FTS HF
477 southern hemisphere VMRs at ~30-35 km in January 2010 with those in the northern
478 hemisphere in July 2010.

479 In addition to side-by-side comparisons of model and observation, the chemistry
480 scheme in SLIMCAT can be tested by comparing (chemically related) tracer-tracer
481 correlations for model and observation; only ACE measurements of fluorine-containing HF
482 ‘precursors’ are available for this purpose. It is widely known that all long-lived species in
483 the stratosphere have compact correlations, even if there is no chemical link between them.
484 As explained by Plumb and Ko (1992), two tracers with lifetimes longer than quasi-
485 horizontal mixing time scales should be in ‘slope equilibrium’ and produce a compact
486 correlation. Species with lifetimes longer than vertical transport time scales will also be in
487 ‘gradient equilibrium’ and the compact correlation will be linear. Furthermore, relative
488 lower-stratospheric lifetimes of long-lived species (with stratospheric sinks via photolysis or
489 reaction with O(¹D)) under gradient equilibrium can be derived from the linear slope of the
490 tracer-tracer correlation (Chipperfield et al., 2014).

491 In the lower stratosphere COF₂ and COCIF can be regarded as long-lived tracers
492 (local lifetimes of many years). Therefore, their tracer isopleths should follow the typical
493 tropopause-following contours of any long-lived tracer. In this sense, COF₂ and COCIF are
494 analogous to NO_y which is produced from N₂O. Figure 4 contains correlation plots between
495 COF₂ and its major source, CFC-12, over the two latitude bands 65-70°S and 65-70°N for
496 two months each over the period September 2009 – August 2010. Comparisons are made at
497 high latitudes, where ACE-FTS observations are more plentiful, and for individual months to
498 ensure that time trends in the source gas VMRs are minimised. The figure reveals that COF₂
499 is indeed long-lived enough to show a good anti-correlation with CFC-12 in the lower
500 stratosphere. Furthermore, agreement between the model and observations is good although
501 there are a few discrepancies around the region of maximum COF₂ VMR; these are due to
502 issues surrounding the scaled a priori used in the retrieval for this altitude region of the
503 profile where the spectral signal has dropped to within the noise level (refer to Harrison et al.
504 (2014) for more details).

505 Figure 5 contains correlation plots between COCIF and its major source, CFC-11,
506 for the same conditions as in Figure 4. Unlike for COF₂ / CFC-12, the agreement between
507 model and ACE-FTS is particularly poor and the model overestimates the peak observed

Deleted: 3

Deleted: 4

Deleted: 3

511 values of COCIF; [this can also be observed in Figure 3](#). There are several possible reasons
512 for this. Firstly, as the modelled VMRs are ~50 % higher than the ACE-FTS VMRs, the
513 modelled COCIF lifetime might be too long, i.e. the model underestimates the COCIF loss
514 processes. This would result in the calculated HF VMRs being slightly lower than they
515 should be, probably by less than a percent, but certainly by less than the uncertainty of the
516 ACE-FTS measurements. An additional SLIMCAT calculation with the COCIF lifetime
517 lowered by a third does improve the agreement with observations. Secondly, the COCIF
518 sources might be overestimated, however SLIMCAT calculations for CFC-11 reveal good
519 agreement with ACE-FTS observations, generally within 10% (Brown et al., 2011).
520 Additionally, the chemistry could be more complicated with additional destruction routes
521 missing from the model. Lastly, there could be a problem with the ACE-FTS retrieval itself.
522 The COCIF linelist used in the ACE-FTS retrieval was taken from the ATMOS database and
523 is described in the literature as ‘very crude’ (Perrin et al., 2011). At the time v3.0 data were
524 first released, this was the best linelist available, however a new and improved linelist has
525 subsequently been generated (Perrin et al., 2011), in which the band intensities are taken
526 from quantum-mechanical calculations. ACE-FTS COCIF retrievals for a handful of
527 occultations have been carried out using the new linelist, however there is no improvement in
528 the disagreement with SLIMCAT.

529 It is expected that the sum of all fluorine source gas VMRs (not including those
530 which have very long lifetimes compared with the period of observations, e.g. CF₄ and SF₆)
531 is anti-correlated with total F_y VMR (HF + 2COF₂ + COCIF) in a conservative way (i.e. the
532 total adds up to a constant). As the ACE-FTS does not measure every source gas, and some
533 minor species have known biases (Brown et al., 2011), we only compare total F_y against the
534 sum of the major source gases, taken as CFC-11, CFC-12, and HCFC-22. The good
535 agreement between plots for SLIMCAT and ACE-FTS (see [Figure 6](#)) confirms that the
536 discrepancy in modelled and retrieved COCIF VMRs has a minimal effect on the overall
537 agreement between model and observation for HF.

538

539 6. Trends

540 Since HF has no chemical sink, with only minor losses arising from rainout in the
541 troposphere and photolysis in the mesosphere, and since the atmosphere contains many long-
542 lived fluorine source gases, the overall HF atmospheric abundance has been increasing for
543 many years and is expected to increase in the foreseeable future. In this section trends in
544 ACE-FTS, HALOE, GOZCARDS and SLIMCAT time series are quantified as a function of

Deleted: 5

546 altitude and latitude. A number of previous studies have quantified trends; for example, a
547 linear trend of $8.5 \pm 1.0\%/year$ (1977 to 1986) (Zander et al., 1987) and $0.48 \pm 0.25\%/year$
548 (2000 to 2009) (Kohlhepp et al., 2012) in total columns measured at Jungfraujoch (46.5°N
549 latitude, 8.0°E longitude), and $0.74 \pm 0.2 \%/year$ (between 30°S and 30°N) derived from
550 ACE-FTS data for 2004 to 2010 (Brown et al., 2011).

551 Prior to the calculation of ACE-FTS, HALOE, and SLIMCAT trends, we derived
552 time series as a function of altitude (on the ACE-FTS grid) and latitude (in 10° bins). Figure
553 7 illustrates the ACE-FTS, HALOE and SLIMCAT time series for HF between 1991 and
554 2013 at selected altitudes for six of the latitude bins; for ease of viewing, error bars are not
555 shown. The annual cycle is clearly visible in each time series, a result of the seasonality of
556 the main ‘source’, COF₂ (Harrison et al., 2014), and careful inspection of Figure 7 reveals
557 that as expected the phase of this cycle is opposite in each hemisphere. The amplitude is
558 largest at high southern latitudes (note the maxima at 29.5 km for the 60° - 70°S plot), due to
559 the descent of HF-rich air in southern winter polar vortices. Note also evidence of the quasi-
560 biennial oscillation (QBO) signal in the tropical plots.

561 Overall the agreement between SLIMCAT and observations presented in Figure 7 is
562 good, however obvious biases are present. In Section 5 it was discussed that ACE v3.0 is
563 biased high relative to HALOE by ~10%. HALOE VMRs are biased low relative to
564 SLIMCAT, generally by between ~5 and 15 %, although SLIMCAT is biased low relative to
565 HALOE by up to ~20 % between ~20 and 30 km in the 0-30°N region. Additionally, there is
566 a discrepancy in the observed and calculated annual cycle structure over the tropics, e.g. 10° -
567 20°N at 34.5 km. In terms of bias, ACE-FTS v3.0/3.5 data generally agree with SLIMCAT
568 to within $\pm 5 \%$, except over much of the lower stratosphere (below 30 km) where SLIMCAT
569 is biased low by at least ~5-15 %, peaking at ~20 % in the 0-30°N region and ~25-35 % at
570 the southern and northern high latitudes (poleward of 50°).

571 Figure 8 illustrates the GOZCARDS and SLIMCAT time series for HF plotted in the
572 same manner as Figure 7. Recall that the GOZCARDS HF data product is a merging of the
573 HALOE v19 and ACE-FTS v2.2 HF datasets, with the relative bias between the datasets
574 removed. The agreement between SLIMCAT and the HALOE component of GOZCARDS
575 above ~30 km is reasonably good, however at lower altitudes there are several regions in
576 which the low bias of SLIMCAT is significantly larger than presented in Figure 7, in
577 particular below 20 km near the south pole, and between ~20 and 30 km in the northern
578 hemisphere, where the bias peaks at ~35 % in the 0-30°N region. The ACE-FTS component
579 of GOZCARDS generally agrees with SLIMCAT to within $\pm 5 \%$ above 30 km at the tropics

Deleted: 6

Deleted: 6

Deleted: 6

Deleted: 1

Deleted: 7

Deleted: 6

Deleted: 6

587 and above 25 km in the polar regions. At altitudes lower than these SLIMCAT is biased low,
 588 for example by ~5 – 10 % at latitudes above 50 °N and up to 25 % lower between 20 and 30
 589 km in the 0-30°N region.

590 The GOZCARDS merging process for HF relied only on the relative bias between
 591 the HALOE v19 HF and ACE-FTS v2.2 HF datasets. In this study, it is not possible to
 592 comment on systematic or absolute biases. However, regardless of the absolute biases of the
 593 various datasets, it is clear that SLIMCAT tends to consistently underestimate HF VMRs at
 594 low altitudes (below 30 km at the tropics and 25 km at the poles) relative to those at higher
 595 altitudes.

596 HF trends for the ACE-FTS, HALOE, and SLIMCAT time series (trends were not
 597 considered for GOZCARDS as this is a merged dataset directly related in a multiplicative
 598 fashion to the original datasets) at each altitude within each latitude bin have been calculated
 599 for three time periods from monthly percentage anomalies in HF zonal means, $C^{z,\theta}(n)$,
 600 defined as

$$601 \quad C^{z,\theta}(n) = 100 \frac{VMR^{z,\theta}(n) - \sum_{m=1}^{12} \delta_{nm} \overline{VMR}^{z,\theta}(m)}{\sum_{m=1}^{12} \delta_{nm} \overline{VMR}^{z,\theta}(m)}, \quad (7)$$

602 where n is a running index from month zero to month $n-1$, $VMR^{z,\theta}(n)$ is the corresponding
 603 mixing ratio at altitude z and latitude θ , $\overline{VMR}^{z,\theta}(m)$ is the average of all zonal means for each
 604 of the twelve months, m , and δ_{nm} , although not used in its strict mathematical sense, is one
 605 when index n corresponds to one of the months m and is zero otherwise (Harrison et al.,
 606 2014). Such an approach essentially removes the annual cycle and the effect of biases in
 607 VMRs; the trend, in units of %/year, is simply equated to the ‘slope’ of the linear regression
 608 between $C^{z,\theta}(n)$ and the dependent variable $n/12$. The inclusion of additional terms such as
 609 the annual cycle and its harmonics resulted in no additional improvement in the regression.
 610 The three time periods considered are January 2004 to December 2012 (ACE-FTS,
 611 SLIMCAT), October 1991 to December 1997 (HALOE, SLIMCAT), and January 1998 to
 612 November 2005 (HALOE, SLIMCAT). The HALOE time series was split into two periods
 613 for which HF growth could be modelled linearly. Errors have been explicitly treated in the
 614 linear regression of the ACE and HALOE data, but not the SLIMCAT outputs.

615 Figure 9 presents the trends in the growth of HF (percent per year) (January 2004 to
 616 December 2012) for ACE and SLIMCAT as a function of latitude and altitude, up to the top
 617 of the ACE-FTS retrieval range. The ACE-FTS plot in Figure 9 indicates that between 2004

Deleted: Had v3.0/v3.5 ACE data been used instead, the GOZCARDS dataset would have been shifted lower in VMR by several percent. Development of v4.0, which will use an improved CO₂ a priori VMR profile for PT retrievals thus improving the accuracy of trends, is currently underway; it is too early to say how v4.0 HF will compare to the earlier versions (C.D. Boone, personal communication, 2015).

Deleted: GOZCARDS HF product relative to SLIMCAT

Deleted: 8

Deleted: 8

628 and 2012, HF has increased most rapidly (2 – 3 %/year) at altitudes below ~25 km in the
629 northern hemisphere and at ~35 km near the equator. Similarly, HF has decreased most
630 rapidly in the southern hemisphere below ~35 km and in the northern hemisphere between ~
631 30 and 35 km. The SLIMCAT plot in the second panel contains a number of features which
632 agree well with those in the ACE plot. In particular, note the region of negative trends in the
633 southern hemisphere below ~30 – 35 km, peaking at -3.5 – -4.0 %/year, the region of high
634 positive trends in the northern hemisphere below ~30 km, peaking at 4.5 – 5.0 %/year, the
635 small region of positive trend at ~35 km near the equator, peaking at 2.0 – 2.5 %/year, and
636 the slightly larger region of negative trend at ~30 – 40 km at 0° to 30°N, peaking at -1.0 – -
637 1.5 %/year. However, the magnitudes of the SLIMCAT trends in the lower stratosphere are
638 biased high compared with the ACE measurements.

639 An additional SLIMCAT run has been performed with dynamics arbitrarily annually
640 repeating those for the year 2000; results from this run give a ‘clean’ HF signal without the
641 complication of changes in stratospheric dynamics. Results from this run are included in the
642 times series plots in Figure 7; the annual repetition in dynamical structure reveals a clearer
643 signal of the long-term chemical changes. ‘Clean’ HF trends for 2004 – 2012 calculated in
644 the same manner as before are plotted in the lowest panel of Figure 9, revealing trends
645 distributed relatively uniformly throughout the stratosphere with values between 0 and 1
646 %/year. This indicates that the variations in trends observed for the full SLIMCAT run result
647 from changes in stratospheric dynamics over the observation period. The information on
648 stratospheric circulation is provided solely by the analyses used to force the SLIMCAT
649 calculations. Similar changes due to stratospheric dynamics were observed for COF₂
650 (Harrison et al., 2014). Moreover, Ploeger et al. (2015) used a Lagrangian chemical transport
651 model, also forced by ECMWF ERA-Interim reanalyses, to look at variations in stratospheric
652 age-of-air (AoA) over the period 1988-2013. They compared their model results with
653 estimates derived from MIPAS satellite observations for 2002-2012. During the period of
654 MIPAS observations they found that stratospheric AoA decreased in the lower stratosphere
655 but showed interhemispheric differences in the trend above about 20 km. Also, despite the
656 ongoing monotonic decrease of near-surface chlorine source gases, recent ground-based and
657 satellite remote-sensing measurements have shown a significant increase in hydrogen
658 chloride (HCl), the main stratospheric chlorine reservoir, in the lower stratosphere of the
659 Northern Hemisphere between 2007 and 2011 (Mahieu et al., 2014). By comparison to
660 similar SLIMCAT simulations as used here, this trend ‘anomaly’ was attributed to multiyear
661 variability in the stratospheric circulation and dynamics.

Deleted: s

Deleted: and 7

Deleted: ‘clean’

Deleted: above

Deleted: 8

Deleted: T

668 Together, the studies discussed above paint a consistent picture whereby variability
669 in stratospheric transport, which varies with altitude and hemisphere, significantly modifies
670 the observed trends in long-lived tracers. This variability seems to be well captured by
671 reanalysis products such as ERA-Interim. Even if these tracers have monotonic VMR trends
672 in the troposphere, this dynamical variability can lead to complicated behaviour in the
673 stratosphere and must therefore be accounted for when using observations to determine
674 underlying chemical trends. A detailed analysis of the changing stratospheric dynamics that
675 are responsible for the observed trends in HF and other species is beyond the scope of this
676 work and would require a coupled chemistry-dynamical model.

677 Trends have similarly been derived for the two HALOE periods. HALOE plots
678 corresponding to the ACE-FTS plots in Figure 9, can be found in Figures 10 (1991 – 1997)
679 and 11 (1998 – 2005). The HALOE trends in Figure 10 peaking in the northern hemisphere
680 between 0° and 40°N broadly agree with those calculated by SLIMCAT in the same region,
681 however SLIMCAT calculates smaller trends at the lowest altitudes and generally
682 underestimates the trends in the southern hemisphere. The differences between the full and
683 fixed-dynamics SLIMCAT runs show the impact of dynamical variability; the fixed-
684 dynamics run provides a clean chemical signal. Of the three periods considered, the
685 comparison between 1991 – 1997 HALOE trends and those calculated from SLIMCAT is the
686 poorest. The North-South asymmetry in trends for the full SLIMCAT calculation, which
687 does not agree with observations, must be due to dynamical variability in the model, with the
688 dynamics imposed solely by the ECMWF analyses. Over the measurement period, the
689 quality of these analyses may vary depending on the available datasets used for the
690 assimilation, but it is very difficult to test how realistic the stratospheric transport is. There
691 are only a handful of other height-resolved datasets that test this aspect of the stratospheric
692 circulation, e.g. ozone (Dhomse et al., 2015). As evidenced by Figure 11, however, the
693 HALOE trends for 1998 – 2005 agree better with SLIMCAT than for the 1991 – 1997 period,
694 with ‘background’ trends generally between 0.5 and 1.5 %/year. In fact, there is very little
695 variability over the majority of the plotted range.

696 Overall global trends in HF, weighted at each altitude and latitude by $\cos^2(\text{latitude}^\circ)$
697 and the average VMR, have been calculated from the three time series using errors
698 determined from the linear regression; these trends are listed in Table 5. The observed HF
699 trends reveal a substantial slowing down in the rate of increase of HF by ~90 % from the
700 mid-1990s over the next 15 years, namely from 4.97 ± 0.12 %/year (1991-1997) to $1.12 \pm$
701 0.08 %/year (1998-2005) to 0.52 ± 0.03 %/year (2004-2012). In addition to direct

Formatted: Indent: First line: 1.5 cm

Deleted: 8

Deleted: 9

Deleted: 0

Deleted: 9

Deleted: 0

707 stratospheric ozone recovery (e.g. Chipperfield et al., 2015), this marked decline in the
708 growth rate of HF is a particularly important marker for the success of the Montreal Protocol,
709 and should drop even further once HCFC-22 is phased out in developing countries over the
710 coming years. Global trends calculated by SLIMCAT for the HALOE (1998 – 2005) and
711 ACE-FTS (2004 – 2012) time series, 1.10 %/year and 0.48 %/year, respectively, agree very
712 well with observations, however for the 1991 – 1997 HALOE period the model produces a
713 value ~20 % lower (4.01 %/year). Again, the reason for this is not completely clear, but is
714 likely related to the ECMWF analysis used to drive the dynamics in the SLIMCAT
715 calculation.

716

717 **7. Conclusions**

718 Hydrogen fluoride (HF) is the most abundant fluorine reservoir in the stratosphere
719 with main sources arising from the atmospheric degradation of CFC-12 (CCl_2F_2), CFC-11
720 (CCl_3F), HCFC-22 (CHClF_2), and CFC-113 ($\text{CCl}_2\text{FCClF}_2$), ozone-depleting species whose
721 emissions are anthropogenic. Monitoring the growth of stratospheric HF is therefore an
722 important marker for the success of the Montreal Protocol.

723 Global distributions and trends of stratospheric HF have been determined from
724 ACE-FTS (2004 –) and HALOE (1991 – 2005) data. Based on the overlap period between
725 datasets, ACE-FTS HF measurements are biased high by ~10% relative to HALOE. The
726 observations have been compared with the output of SLIMCAT, a three-dimensional CTM,
727 and the agreement is generally good, although SLIMCAT tends to underestimate HF VMRs
728 at low altitudes (below 30 km at the tropics and 25 km at the poles) relative to those at higher
729 altitudes.

Deleted: .

730 The observed global HF trends reveal a substantial slowing down in the rate of
731 increase of HF since the 1990s: 4.97 ± 0.12 %/year (1991-1997; HALOE), 1.12 ± 0.08
732 %/year (1998-2005; HALOE), and 0.52 ± 0.03 %/year (2004-2012; ACE-FTS), indicating
733 the effectiveness of the Montreal Protocol in phasing out the principal precursor species. For
734 the same periods, SLIMCAT calculates trends of 4.01 %/year, 1.10 %/year, and 0.48 %/year,
735 respectively. The observations also reveal variations in the HF trends with latitude and
736 altitude, for example between 2004 and 2012 HF actually decreased in the southern
737 hemisphere below ~35 km. SLIMCAT calculations broadly agree with these observations,
738 most notably between 2004 and 2012. Such variations are attributed to variability in
739 stratospheric dynamics over the observation period.

741 The ACE-FTS is the only satellite instrument currently making measurements of
742 HF, and continues to operate with only minor loss in performance since its launch. It will
743 therefore be possible to extend the HF time series to the present day and beyond, and
744 subsequently extend the comparison with SLIMCAT.

745

746 **Author contribution**

747 J. J. Harrison devised the study and performed the data analysis. C. D. Boone and P.
748 F. Bernath provided the ACE-FTS data. J. Russell III provided the HALOE HF data. L.
749 Froidevaux and J. Anderson provided the HF GOZCARDS data. M. P. Chipperfield and S.
750 S. Dhomse ran the SLIMCAT model and provided additional explanation of the outputs. J. J.
751 Harrison prepared the manuscript with contributions from M. P. Chipperfield and the other
752 co-authors.

753

754 **Acknowledgements**

755 The authors wish to thank the UK Natural Environment Research Council (NERC)
756 for supporting J. J. Harrison through grant NE/I022663/1 and through the National Centre for
757 Earth Observation (NCEO). The ACE satellite mission is funded primarily by the Canadian
758 Space Agency (CSA). HALOE was funded by NASA. M. P. Chipperfield and S. S. Dhomse
759 thank Wuhu Feng (the National Centre for Atmospheric Science; NCAS) for help with
760 SLIMCAT. M. P. Chipperfield is a Royal Society Wolfson Research Merit Award holder.
761 Work at the Jet Propulsion Laboratory was performed under contract with the National
762 Aeronautics and Space Administration (NASA).

763

764 **Figure Captions**

765

766 **Figure 1.** A comparison between ACE-FTS and SLIMCAT HF zonal means (September
767 2009 to August 2010). A full discussion of the seasonal variation in the HF distribution is
768 provided in the text.

769

770 **Figure 2.** A comparison between ACE-FTS, HALOE and SLIMCAT HF zonal means
771 (September 2004 to August 2005). The ACE-FTS and HALOE time series of measurements
772 overlap during the period January 2004 to November 2005.

773

774 **Figure 3.** A comparison of COF₂ and COCIF zonal means from ACE-FTS and SLIMCAT
775 for October 2009, and February and August 2010.

Deleted:)

776
777 **Figure 4.** Correlation plots between coincident CFC-12 and COF₂ ACE-FTS observations
778 and SLIMCAT calculations for November 2009 / July 2010 65-70°S and January / May 2010
779 65-70°N. The error bars represent the standard deviations in the ACE-FTS VMRs.

Deleted: 3

780
781 **Figure 5.** Correlation plots between coincident CFC-11 and COCIF ACE-FTS observations
782 and SLIMCAT calculations for November 2009 / July 2010 65-70°S and January / May 2010
783 65-70°N. The error bars represent the standard deviations in the ACE-FTS VMRs.

Deleted: 4

784
785 **Figure 6.** Correlation plots between coincident ACE-FTS observations and SLIMCAT
786 calculations of total 'major' organic fluorine, based on CFC-11, CFC-12, and HCFC-22, and
787 total inorganic fluorine, F_y, for November 2009 / July 2010 65-70°S and January / May 2010
788 65-70°N. The error bars represent the standard deviations in the ACE-FTS VMRs.

Deleted: 5

789
790 **Figure 7.** The HALOE, ACE-FTS and SLIMCAT HF time series for selected altitude –
791 latitude bin combinations. Observations are plotted between October 1991 and December
792 2012. Overlaid are the time series from a SLIMCAT run with dynamics arbitrarily annually
793 repeating those for the year 2000; this provides a clearer signal of the long-term chemical
794 changes without the complication of variations in stratospheric dynamics.

Deleted: 6

Deleted: changes

795
796 **Figure 8.** The GOZCARDS and SLIMCAT HF time series for selected altitude – latitude bin
797 combinations. Observations are plotted between October 1991 and September 2010.

Deleted: ¶

Deleted: 7

798
799 **Figure 9.** Trends in the growth of HF (% yr⁻¹; January 2004 to December 2012) for ACE-
800 FTS and SLIMCAT as a function of latitude and altitude. A full discussion of these trends is
801 provided in the text.

Deleted: 8

802
803 **Figure 10.** Trends in the growth of HF (% yr⁻¹; October 1991 to December 1997) for
804 HALOE and SLIMCAT as a function of latitude and altitude. A full discussion of these
805 trends is provided in the text.

Deleted: 9

806

817 **Figure 11.** Trends in the growth of HF (% yr⁻¹; January 1998 to November 2005) for
818 HALOE and SLIMCAT as a function of latitude and altitude. A full discussion of these
819 trends is provided in the text.

Deleted: 0

820

821 **References**

822

823 Bernath, P. F., McElroy, C. T., Abrams, M. C., Boone, C. D., Butler, M., Camy-Peyret, C.,
824 Carleer, M., Clerbaux, C., Coheur, P.-F., Colin, R., DeCola, P., DeMazière, M., Drummond,
825 J. R., Dufour, D., Evans, W. F. J., Fast, H., Fussen, D., Gilbert, K., Jennings, D.E.,
826 Llewellyn, E. J., Lowe, R. P., Mahieu, E., McConnell, J. C., McHugh, M., McLeod, S. D.,
827 Michaud, R., Midwinter, C., Nassar, R., Nichitiu, F., Nowlan, C., Rinsland, C. P., Rochon, Y.
828 J., Rowlands, N., Semeniuk, K., Simon, P., Skelton, R., Sloan, J. J., Soucy, M.-A., Strong,
829 K., Tremblay, P., Turnbull, D., Walker, K. A., Walkty, I., Wardle, D. A., Wehrle, V., Zander,
830 R., and Zou, J.: Atmospheric Chemistry Experiment (ACE): Mission overview, *Geophys.*
831 *Res. Lett.*, 32, L15S01, doi:10.1029/2005GL022386, 2005.

832

833 Boone, C. D., Walker, K. A., Bernath, P. F.: Version 3 Retrievals for the Atmospheric
834 Chemistry Experiment Fourier Transform Spectrometer (ACE-FTS). In *The Atmospheric*
835 *Chemistry Experiment ACE at 10: A Solar Occultation Anthology*; Bernath, P. F., Ed.; A.
836 Deepak Publishing, Hampton, Virginia, U.S.A., 103-127, 2013. Available at
837 <http://www.ace.uwaterloo.ca/publications/2013/Version3.5retrievals2013.pdf>.

Deleted: <http://acebox2.uwaterloo.ca/publications/2013/Version3.5retrievals2013.pdf>

838

839 Brown, A. T., Chipperfield, M. P., Boone, C., Wilson, C., Walker, K. A., Bernath, P. F.:
840 Trends in atmospheric halogen containing gases since 2004, *J. Quant. Spectrosc. Rad. Trans.*,
841 112, 2552-2566, 2011.

842

843 Brown, A. T., Chipperfield, M. P., Richards, N. A. D., Boone, C., and Bernath, P. F.: Global
844 stratospheric fluorine inventory for 2004–2009 from Atmospheric Chemistry Experiment
845 Fourier Transform Spectrometer (ACE-FTS) measurements and SLIMCAT model
846 simulations, *Atmos. Chem. Phys.*, 14, 267-282, doi:10.5194/acp-14-267-2014, 2014.

847

848 Chipperfield, M. P.: Multiannual simulations with a three-dimensional chemical transport
849 model, *J. Geophys. Res.*, 104, 1781–1805, doi:10.1029/98jd02597, 1999.

850

854 Chipperfield, M. P.: New version of the TOMCAT/SLIMCAT off-line chemical transport
855 model: Intercomparison of stratospheric tracer experiments, *Q. J. R. Meteorol. Soc.*, 132,
856 1179–1203, 2006.

857

858 Chipperfield, M. P., Liang, Q., Strahan, S. E., Morgenstern, O., Dhomse, S. S., Abraham, N.
859 L., Archibald, A. T., Bekki, S., Braesicke, P., Di Genova, G., Fleming, E. L., Hardiman, S.
860 C., Iachetti, D., Jackman, C. H., Kinnison, D. E., Marchand, M., Pitari, G., Pyle, J. A.,
861 Rozanov, E., Stenke, A., Tummon, F.: Multimodel estimates of atmospheric lifetimes of
862 long-lived ozone-depleting substances: Present and future, *J. Geophys. Res. Atmos.*, 119,
863 2555–2573, doi:10.1002/2013JD021097, 2014.

864

865 Chipperfield, M.P., Dhomse, S.S., Feng, W., McKenzie, R.L., Velders, G., Pyle, J.A.:
866 Quantifying the ozone and UV benefits already achieved by the Montreal Protocol, *Nature*
867 *Communications*, 6, 7233, doi:10.1038/ncomms8233, 2015.

868

869 Connor, B. J., and Rodgers, C. D.: A comparison of retrieval methods: Optimal estimation,
870 onion peeling, and a combination of the two, in *RSRM 1987: Advances in Remote Sensing*
871 *Retrieval Methods*; edited by Deepak, A., Fleming, H. E., and Theon, J. S., Eds.; A. Deepak
872 Publishing, Hampton, Virginia, U.S.A., 1989.

873

874 Dhomse, S., Chipperfield, M.P., Feng, W., Hossaini, R., Mann, G.W., Santee, M.L.:
875 Revisiting the hemispheric asymmetry in mid-latitude ozone changes following the Mount
876 Pinatubo eruption: A 3-D model study, *Geophys. Res. Lett.*, 42, 3038-3047,
877 doi:10.1002/2015GL063052, 2015.

878

879 Duchatelet, P., Demoulin, P., Hase, F., Ruhnke, R., Feng, W., Chipperfield, M. P., Bernath,
880 P. F., Boone, C. D., Walker, K. A., and Mahieu, E.: Hydrogen fluoride total and partial
881 column time series above the Jungfraujoch from long-term FTIR measurements: Impact of
882 the line-shape model, characterization of the error budget and seasonal cycle, and comparison
883 with satellite and model data, *J. Geophys. Res.*, 115, D22306, doi:10.1029/2010JD014677,
884 2010.

885

886 Feng, W., Chipperfield, M. P., Dorf, M., Pfeilsticker, K., and Ricaud, P.: Mid-latitude ozone
887 changes: studies with a 3-D CTM forced by ERA-40 analyses, *Atmos. Chem. Phys.*, 7, 2357–
888 2369, doi:10.5194/acp-7-2357-2007, 2007.

889

890 Froidevaux, L., Anderson, J., Wang, H.-J., Fuller, R. A., Schwartz, M. J., Santee, M. L.,
891 Livesey, N. J., Pumphrey, H. C., Bernath, P. F., Russell III, J. M., and McCormick, M. P.:
892 Global OZone Chemistry And Related trace gas Data records for the Stratosphere
893 (GOZCARDS): methodology and sample results with a focus on HCl, H₂O, and O₃, *Atmos.*
894 *Chem. Phys.*, 15, 10471-10507, doi:10.5194/acp-15-10471-2015, 2015.

895

896 Fu, D., Boone, C. D., Bernath, P. F., Weisenstein, D. K., Rinsland, C. P., Manney, G. L.,
897 Walker, K. A. First global observations of atmospheric COClF from the Atmospheric
898 Chemistry Experiment mission, *J. Quant. Spectrosc. Rad. Trans.*, 110, 974–985, 2009.

899

900 Gribble, G. W. Naturally Occurring Organofluorines. In *Handbook of Environmental*
901 *Chemistry*, Vol.3, Part N: Organofluorines; Neilson, A. H., Ed.; Springer-Verlag: Berlin
902 Heidelberg, 2002.

903

904 Harrison, J. J., Chipperfield, M. P., Dudhia, A., Cai, S., Dhomse, S., Boone, C. D., and
905 Bernath, P. F.: Satellite observations of stratospheric carbonyl fluoride, *Atmos. Chem. Phys.*,
906 14, 11915-11933, doi:10.5194/acp-14-11915-2014, 2014.

907

908 Irion F.W., Gunson M.R., Toon G.C., Chang A.Y., Eldering A., Mahieu E., Manney G.L.,
909 Michelsen H.A., Moyer E.J., Newchurch M.J., Osterman G.B., Rinsland C.P., Salawitch R.J.,
910 Sen B., Yung Y.L., Zander R., *Atmospheric Trace Molecule Spectroscopy (ATMOS)*
911 *Experiment Version 3 data retrievals*, *Appl Opt.* 2002 Nov 20;41(33):6968-79.

912

913 Kohlhepp, R., Ruhnke, R., Chipperfield, M. P., De Mazière, M., Notholt, J., Barthlott, S.,
914 Batchelor, R. L., Blatherwick, R. D., Blumenstock, Th., Coffey, M. T., Demoulin, P., Fast,
915 H., Feng, W., Goldman, A., Griffith, D. W. T., Hamann, K., Hannigan, J. W., Hase, F.,
916 Jones, N. B., Kagawa, A., Kaiser, I., Kasai, Y., Kirner, O., Kouker, W., Lindenmaier, R.,
917 Mahieu, E., Mittermeier, R. L., Monge-Sanz, B., Morino, I., Murata, I., Nakajima, H., Palm,
918 M., Paton-Walsh, C., Raffalski, U., Reddmann, Th., Rettinger, M., Rinsland, C. P., Rozanov,
919 E., Schneider, M., Senten, C., Servais, C., Sinnhuber, B.-M., Smale, D., Strong, K.,

920 Sussmann, R., Taylor, J. R., Vanhaelewyn, G., Warneke, T., Whaley, C., Wiehle, M., and
921 Wood, S. W.: Observed and simulated time evolution of HCl, ClONO₂, and HF total column
922 abundances, *Atmos. Chem. Phys.*, 12, 3527-3556, doi:10.5194/acp-12-3527-2012, 2012.

923

924 Mahieu, E., Duchatelet, P., Demoulin, P., Walker, K. A., Dupuy, E., Froidevaux, L., Randall,
925 C., Catoire, V., Strong, K., Boone, C. D., Bernath, P. F., Blavier, J.-F., Blumenstock, T.,
926 Coffey, M., De Mazière, M., Griffith, D., Hannigan, J., Hase, F., Jones, N., Jucks, K. W.,
927 Kagawa, A., Kasai, Y., Mebarki, Y., Mikuteit, S., Nassar, R., Notholt, J., Rinsland, C. P.,
928 Robert, C., Schrems, O., Senten, C., Smale, D., Taylor, J., Tétard, C., Toon, G. C., Warneke,
929 T., Wood, S. W., Zander, R., and Servais, C.: Validation of ACE-FTS v2.2 measurements of
930 HCl, HF, CCl₃F and CCl₂F₂ using space-, balloon- and ground-based instrument
931 observations, *Atmos. Chem. Phys.*, 8, 6199-6221, doi:10.5194/acp-8-6199-2008, 2008.

932

933 Mahieu, E., Chipperfield, M. P., Notholt, J., Reddman, T., Anderson, J., Bernath, P. F.,
934 Blumenstock, T., Coffey, M. T., Dhomse, S. S., Feng, W., Franco, B., Froidevaux, L.,
935 Griffith, D. W. T., Hannigan, J. W., Hase, F., Hossaini, R., Jones, N. B., Morino, I., Murata,
936 I., Nakajima, H., Palm, M., Paton-Walsh, C., Russell III, J. M., Schneider, M., Servais, C.,
937 Smale, D., and Walker, K. A: Recent Northern Hemisphere stratospheric HCl increase due to
938 atmospheric circulation changes, *Nature*, 515, 104-107, doi:10.1038/nature13857, 2014.

939

940 Monge-Sanz, B. M., Chipperfield, M. P., Simmons, A. J., and Uppala, S. M.: Mean age of air
941 and transport in a CTM: Comparison of different ECMWF analyses, *Geophys. Res. Lett.*, 34,
942 L04801, doi:10.1029/2006gl028515, 2007.

943

944 Perrin, A., Demaison, J., and Toon, G.: The ν_1 , ν_2 , and ν_3 bands of carbonyl chlorofluoride
945 (COFCl) at 5.3, 9.1, and 13.1 μm : position and intensity parameters and their use for
946 atmospheric studies, *J. Quant. Spectrosc. Rad. Trans.*, 112, 1266-1279,
947 10.1016/j.jqsrt.2011.01.003, 2011.

948

949 [Ploeger, F., Riese, M., Haenel, F., Konopka, P., Müller, R. and Stiller, G.: Variability of](#)
950 [stratospheric mean age of air and of the local effects of residual circulation and eddy mixing.](#)
951 [J. Geophys. Res. Atmos., 120, 716–733, doi:10.1002/2014JD022468, 2015.](#)

952

953 Plumb, R. A. and Ko, M. K. W.: Interrelationships between mixing ratios of long-lived
954 stratospheric constituents, *J. Geophys. Res.*, 97, 10145–10156, 1992.
955
956 Ricaud, P., and Lefevre, F.: Fluorine in the atmosphere. In *Fluorine and the Environment:
957 Atmospheric Chemistry, Emissions, & Lithosphere*; Tressaud, A., ed., Elsevier, 2006.
958
959 Rothman, L.S., Gamache, R.R., Tipping, R.H., Rinsland, C.P., Smith, M.A.H., Benner D. C.,
960 Devi, V.M, Flaud, J.-M., Camy-Peyret, C., Perrin, A., Goldman, A., Massie, S.T., Brown,
961 L.R., Toth, R.A.: The HITRAN molecular database: Editions of 1991 and 1992, *J. Quant.
962 Spectrosc. Radiat. Transfer*, 48, 469–507, 1992.
963
964 Rothman, L.S., Jacquemart, D., Barbe, A., Benner, C. D., Birk, M., Brown, L. R., Carleer, M.
965 R., Chackerian Jr., C., Chance, K., Coudert, L. H., Dana, V., Devi, V. M., Flaud, J.-M.,
966 Gamache, R. R., Goldman, A., Hartmann, J.-M., Jucks, J. W., Maki, A. G., Mandin, J.-Y.,
967 Massie, S. T., Orphal, J., Perrin, A., Rinsland, C. P., Smith, M., Tennyson, J., Tolchenov, R.
968 N., Toth, R. A., Vander Auwera, J., Varanasi, P., and Wagner, G.: The HITRAN 2004
969 molecular spectroscopic database, *J. Quant. Spectrosc. Radiat. Transfer*, 96, 193–204, 2005.
970
971 Rothman, L.S., Gordon, I.E., Babikov, Y., Barbe, A., Benner, D.C., Bernath, P.F., Birk, M.,
972 Bizzocchi, L., Boudon, V., Brown, L.R., Campargue, A., Chance, K., Cohen, E.A., Coudert,
973 L.H., Devi, V.M., Drouin, B.J., Fayt, A., Flaud, J.-M., Gamache, R.R., Harrison, J.J.,
974 Hartmann, J.-M., Hill, C., Hodges, J.T., Jacquemart, D., Jolly, A., Lamouroux, J., Le Roy,
975 R.J., Li, G., Long, D.A., Lyulin, O.M., Mackie, C.J., Massie, S.T., Mikhailenko, S., Müller,
976 H.S.P., Naumenko, O.V., Nikitin, A.V., Orphal, J., Perevalov, V., Perrin, A., Polovtseva,
977 E.R., Richard, C., Smith, M.A.H., Starikova, E., Sung, K., Tashkun, S., Tennyson, J., Toon,
978 G.C., Tyuterev, V.I., Wagner, G.: The HITRAN2012 molecular spectroscopic database, *J.
979 Quant. Spectrosc. Radiat. Transfer*, 130, 4-50, 2013.
980
981 Russell III, J. M., Gordley, L. L., Park, J. H., Drayson, S. R., Hesketh, W. D., Cicerone, R. J.,
982 Tuck, A. F., Frederick, J. E., Harries, J. E., Crutzen, P. J.: The Halogen Occultation
983 Experiment, *J. Geophys. Res.*, 98, 10777-10797, doi:10.1029/93JD00799, 1993.
984
985 Russell III, J. M., Deaver, L. E., Luo, M., Cicerone, R. J., Park, J. H., Gordley, L. L., Toon,
986 G. C., Gunson, M. R., Traub, W. A., Johnson, D. G., Jucks, K. W., Zander, R. and Nolt, I. G.:

987 Validation of hydrogen fluoride measurements made by the Halogen Occultation Experiment
988 from the UARS platform, *J. Geophys. Res.*, 101, 10163–10174, 1996.
989
990 Velazco, V. A., Toon, G. C., Blavier, J.-F. L., Kleinböhl, A., Manney, G. L., Daffer, W. H.,
991 Bernath, P. F., Walker, K. A., and Boone, C.: Validation of the Atmospheric Chemistry
992 Experiment by noncoincident MkIV balloon profiles, *J. Geophys. Res.*, 116, D06306,
993 doi:10.1029/2010jd014928, 2011.
994
995 Zander, R., Roland, G. and Delbouille, L.: Confirming the presence of hydrofluoric acid in
996 the upper stratosphere, *Geophys. Res. Lett.*, 4, 117–120, 1977.
997
998 Zander, R., Roland, G., Delbouille, L., Sauval, A., Farmer, C.B., Norton, R.H.: Monitoring of
999 the integrated column of hydrogen fluoride above the Jungfraujoch Station since 1977 — the
1000 HF/HCl column ratio, *Journal of Atmospheric Chemistry*, 5, 385-394, 1987.
1001
1002

1003 **Tables**

1004

1005 Table 1: Microwindows for the v3.0/v3.5 ACE-FTS hydrogen fluoride retrieval.

Centre Frequency (cm ⁻¹)	Microwindow width (cm ⁻¹)	Lower altitude (km)	Upper altitude (km)
3787.60	1.60	40	2.00E+16 ^b
3788.28	0.60	12	40
3792.65 ^a	0.40	20	40
3833.70	0.80	16	40
3834.30	1.60	40	9.00E+15 ^b
3877.60	0.80	12	9.00E+15 ^b
3920.15	0.70	25	9.00E+15 ^b
4000.87	0.65	12	9.00E+15 ^b
4038.82	1.00	12	9.00E+15 ^b
4075.35	0.80	25	9.00E+15 ^b
4109.75	0.80	25	2.00E+16 ^b

1006 ^a Included to improve results for interferer HDO.

1007 ^b Upper altitude given in atmospheric density units, molecules cm⁻³.

1008

1009

1010 Table 2: Interferers in the v3.0/v3.5 ACE-FTS hydrogen fluoride retrieval.

Molecule	Lower altitude limit (km)	Upper altitude limit (km)
H ₂ O	12	65
H ¹⁸ OH	12	50
H ¹⁷ OH	12	40
HDO	12	25
CO ₂	12	40
O ₃	12	38
CH ₄	12	30
OC ¹⁸ O	12	20
N ₂ O	12	30

1011

1012

1013 Table 3: Sources of systematic uncertainty in the ACE-FTS v3.0/v3.5 hydrogen fluoride
 1014 retrieval.

Source	Symbol	Fractional value
HF spectroscopy	μ_{spec}	0.04
Spectral interferers	μ_{int}	0.01
Temperature	μ_T	0.01
Altitude	μ_z	0.03
ILS	μ_{ILS}	0.09

Deleted: COF₂

1015
 1016 Table 4: Fluorine source gases in the SLIMCAT chemical scheme and their atmospheric
 1017 degradation products.

Source gases		Product gases
Commercial name	Chemical formula	
CFC-11	CCl ₃ F	COCIF
CFC-12	CCl ₂ F ₂	COF ₂
CFC-113	CCl ₂ FCClF ₂	COCIF + COF ₂
CFC-114	CClF ₂ CClF ₂	2COF ₂
CFC-115	CClF ₂ CF ₃	2COF ₂ + HF
HCFC-22	CHClF ₂	COF ₂
HCFC-141b	CH ₃ CCl ₂ F	COCIF
HCFC-142b	CH ₃ CClF ₂	COF ₂
HFC-23	CHF ₃	COF ₂ + HF
HFC-134a	CH ₂ FCF ₃	COF ₂ + 2HF
HFC-152a	CH ₃ CHF ₂	2COF ₂
Halon 1211	CBrClF ₂	COF ₂
Halon 1301	CBrF ₃	COF ₂ + HF
Halon 2402	CBrF ₂ CBrF ₂	4HF
	COCIF ^a	HF
	COF ₂ ^a	2HF

Deleted: ¶

1018 ^a These are not source gases, but their degradation products are included for completion.

1019
 1020 Table 5: Trends ([%/year](#)) derived from the HALOE v19 and ACE-FTS v3.0/v3.5 HF
 1021 observations.

Dataset	Period	Observed trend	SLIMCAT trend
HALOE	1991-1997	4.97 ± 0.12	4.01
HALOE	1998-2005	1.12 ± 0.08	1.10
ACE-FTS	2004-2012	0.52 ± 0.03	0.48

1022